

Many-body effects on the appearance potential spectroscopy of metals

Russell S. Patrick and Shyamalendu M. Bose

Department of Physics and Atmospheric Science, Drexel University, Philadelphia, Pennsylvania 19104

Pierre Longe

Institut de Physique, Batiment 5, Université de Liège, Sart-Tilman, B-4000 Liège, Belgium

(Received 7 April 1986)

The contribution of single-particle excitations to the intensity of the appearance potential spectra (APS) of metals has been calculated. This contribution is found to be finite and smooth away from the edge. The edge structure and the structure at the threshold for plasmon production are not modified by the single-particle contribution. However, the change in concavity in the APS intensity at the plasmon cutoff frequency becomes less pronounced by this contribution.

I. INTRODUCTION

In this report, results of a theoretical study of the effects of electron-electron interactions on the appearance potential spectra (APS) of metals are presented.¹ These interaction effects include plasmon satellites, modification of the main band due to electron-hole production, and the anomalous edge behavior. To describe these effects on the APS, we have used diagrammatic techniques of many-body perturbation theory. Results in regard to the first plasmon satellite² (Ref. 2 is hereafter referred to as I) and the edge structure³ (Ref. 3 is hereafter referred to as II) have already been published. In this paper, we present a calculation of the modification of the APS intensity due to single-particle excitations. These results are then added to those of I and II to obtain a complete description of the effects of electron-electron interactions on APS of metals.

An S - and T -matrix approach, first developed by Longe and co-workers^{4,5} for the study of core-level photoemission spectra, provides a means to calculate the effect of plasmons and particle-hole production on the APS intensity. These effects occur because of scattering of the conduction-band electrons by (a) the incident electron, (b) the core hole, and (c) the two final-state electrons in their flight through the Fermi sea. In addition, the contribution of these effects on the APS is modified by quantum interference between any two of the above processes. A calculation incorporating the above processes has been carried out to first order in the effective Coulomb interaction using the random-phase approximation (RPA) to describe the polarization of the electrons in the metal. However, divergences in the first-order theory require us to include higher-order interaction effects by a renormalization procedure. This renormalization accounts for virtual interactions of a particle with the Fermi sea and is incorporated into our calculations by the use of a self-energy function.

With regard to effects of single particle-hole pair production, the modification of the main band is smooth in regions away from the threshold. Near the threshold, however, a sharp peak is found. The reason for this is that the core hole, unimpaired by momentum conserva-

tion, can create enormous numbers of low-energy particle-hole pairs near the Fermi surface with little expenditure of energy. Attempts to describe this core hole—electron scattering by the S -matrix formalism fail since any perturbation theory of this type is incapable of taking into account such a catastrophic effect. The effect is handled by an extension of the Nozières—De Dominicis (ND)-Laramore edge formalism to the APS.^{6,7}

In the next section, a brief review of the S -matrix and edge formalism used in our calculations is given. In Sec. III, calculated derivative APS curves are presented for the $1s$ and $2p$ APS of aluminum along with a discussion of the results.

II. FORMALISM

Let us consider a semi-infinite metal occupying the region $z \leq 0$ with the surface at $z = 0$. Assuming that the path of the incident electron is normal to the surface and its speed (v_T) is uniform, the total intensity function for an n th-order interaction process is written as

$$I_n(\epsilon_k) = \int_{-\infty}^0 dz \rho(z) J_n(z, \epsilon_k) \\ = v_T \rho \int_0^{\infty} d\tau J_n(\tau, \epsilon_k), \quad (1)$$

where $\rho(z = v_T \tau)$ is the density of core-hole states (assumed constant), τ is time it takes for the incident electron to excite a core hole, and $J_n(\tau, \epsilon_k)$ is the production rate for core-hole excitation. $J_n(\tau, \epsilon_k)$ gives the probability that an incident electron with energy ϵ_k will excite a core hole in time τ . This can be related to the scattering amplitude $S_n(\tau, \epsilon_k)$ by the time-dependent golden rule

$$J_n(\tau, \epsilon_k) = \frac{1}{2\pi t_0 N} \sum_f |S_n(\tau, \epsilon_k)|^2, \quad (2)$$

where the sum is over the final states, t_0 is the observation time for the entire APS process, and N is a normalization factor introduced to ensure conservation of incident electron number. This normalization constant N is obtained from the sum rule

$$\int_0^{\infty} d\epsilon_k \sum_n J_n(\tau, \epsilon_k) = 1. \quad (3)$$

To calculate the scattering amplitude we have used

standard techniques of many-body perturbation theory. Diagrams describing the APS process in the zeroth and first order in the effective interaction are shown in Fig. 1. In the diagrams, a single (heavy) line pointing upwards represents propagation of a bare (renormalized) conduction electron of energy ϵ_p , a double line pointing downward a core hole of energy E_c (<0), and the dashed horizontal line the Coulomb interaction initiating the APS process. The wavy line represents the effective interaction (single-particle or plasmon) with the electron gas in the metal. The S -matrix elements associated with these diagrams in the zeroth and first order are given in I [Eqs. (5) and (13)–(16)].

The intensity function is obtained by inserting the S -matrix elements into (2), then (2) into (1). Squaring the S -matrix elements will result in an extrinsic term, an intrinsic term due to the core hole, intrinsic terms due to the final-state electrons, and cross terms which account for the quantum interference effects. The effective interaction is contained in the electronic coupling function $C(q, \omega_q)$ which is in the transition matrix $U_{II'}$ [see Eq. (17) of I].

The coupling term can be separated into a plasmon

term and single-particle term. Calculations of the plasmon satellite require the insertion of

$$C_{pl}(q, \omega) = [\pi \omega_p(q) V(q)]^{1/2} \delta(\omega - \omega_p(q)) \quad (4)$$

for $C_{pl}(q, \omega)$. In (4), $V(q)$ is the bare Coulomb interaction and $\omega_p(q)$ is the plasmon frequency. The calculation of the APS intensity due to single plasmon excitation has been given in I.

For the single-particle terms, the square of the electronic coupling function takes the form

$$C_{SP}^2 = 2V(q) \text{Im} \left[\frac{-1}{\epsilon(q, \omega_q)} \right], \quad (5)$$

where $\epsilon(q, \omega_q)$ is the frequency-dependent Lindhard dielectric function. Following the same steps as in I with the exception of the different coupling strength the extrinsic, intrinsic due to core hole, intrinsic due to final-state electrons, and cross terms for the intensity can be written as

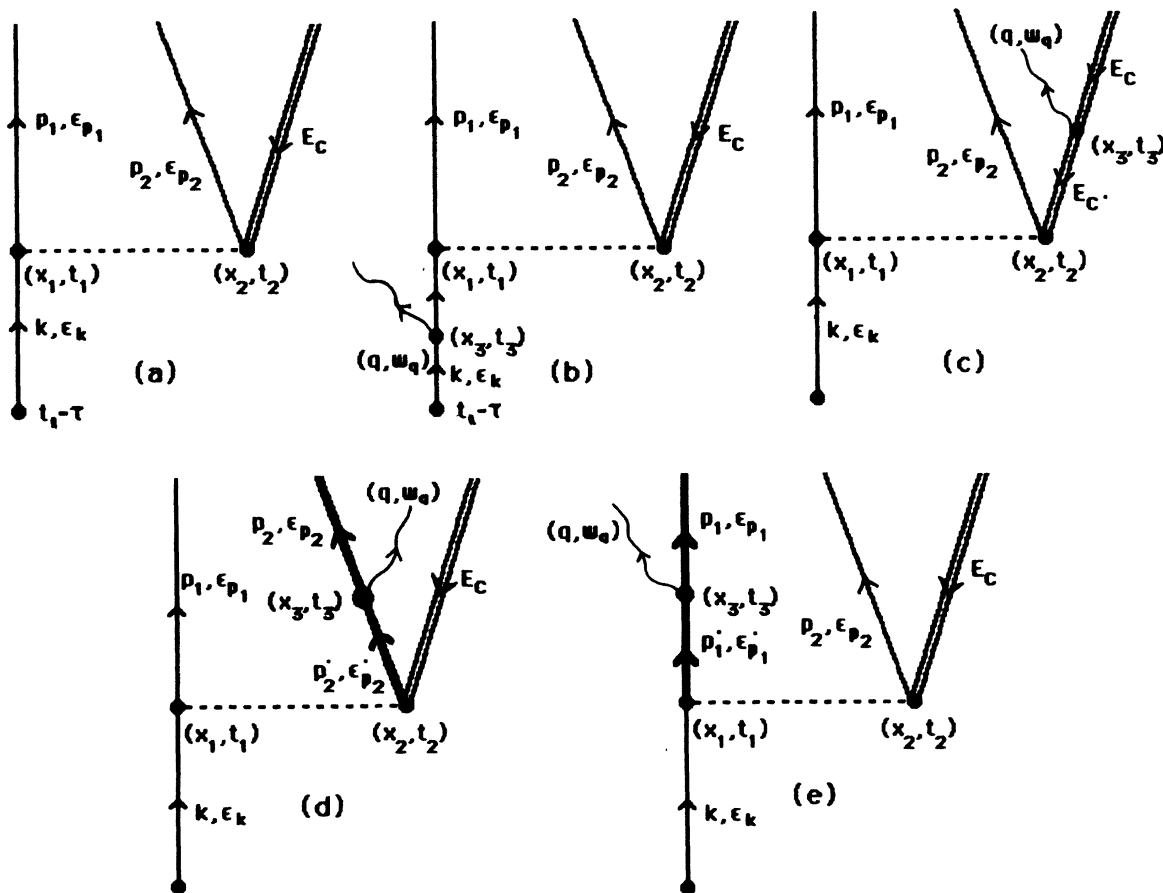


FIG. 1. Diagrams showing the basic APS process in the (a) zeroth and (b)–(e) first order in the effective Coulomb interaction. For the first-order process, (b) is the extrinsic diagram, (c) is the intrinsic term due to the core hole (E_c), and (d) and (e) are the intrinsic terms due to the final-state electrons ($\epsilon_{p_1}, \epsilon_{p_2}$).

$$I_{\text{ext}}(\epsilon_k) \propto \int_{|\mathbf{p}_1| > k_F} d^3 p_1 \int_{|\mathbf{p}_2| > k_F} d^3 p_2 \int d^3 q \int d\omega_q V(q) \text{Im} \left[\frac{-1}{\epsilon(q, \omega_q)} \right] \\ \times \delta(\nu) \delta(\epsilon_k + E_c - \omega_q - \epsilon_{p_1} - \epsilon_{p_2}) \Theta(|\mathbf{k} - \mathbf{q}| - k_F), \quad (6a)$$

$$I_{\text{int}}^{\text{core}}(\epsilon_k) \propto \int_{|\mathbf{p}_1| > k_F} d^3 p_1 \int_{|\mathbf{p}_2| > k_F} d^3 p_2 \int d^3 q \int \frac{d\omega_q}{\omega_q^2} V(q) \text{Im} \left[\frac{-1}{\epsilon(q, \omega_q)} \right] \delta(\epsilon_k + E_c - \omega_q - \epsilon_{p_1} - \epsilon_{p_2}), \quad (6b)$$

$$I_{\text{int}}^{\text{cond}}(\epsilon_k) \propto \int_{|\mathbf{p}_1| > k_F} d^3 p_1 \int_{|\mathbf{p}_2| > k_F} d^3 p_2 \int d^3 q \int d\omega_q V(q) \text{Im} \left[\frac{-1}{\epsilon(q, \omega_q)} \right] \\ \times \delta(\epsilon_k + E_c - \omega_q - \epsilon_{p_1} - \epsilon_{p_2}) \frac{\Theta(|\mathbf{p}_1 + \mathbf{q}| - k_F)}{\mu_1^2 + W_1^2}, \quad (6c)$$

$$I_{\text{cross}}(\epsilon_k) \propto \int_{|\mathbf{p}_1| > k_F} d^3 p_1 \int_{|\mathbf{p}_2| > k_F} d^3 p_2 \int d^3 q \int d\omega_q V(q) \text{Im} \left[\frac{-1}{\epsilon(q, \omega_q)} \right] \delta(\epsilon_k + E_c - \omega_q - \epsilon_{p_1} - \epsilon_{p_2}) \\ \times \left[\frac{2P}{v\omega_q} \Theta(|\mathbf{k} - \mathbf{q}| - k_F) + \frac{4P\mu_1 \Theta(|\mathbf{k} - \mathbf{q}| - k_F) \Theta(|\mathbf{p}_1 + \mathbf{q}| - k_F)}{v(\mu_1^2 + W_1^2)} \right. \\ \left. + \frac{4\mu_1 \Theta(|\mathbf{p}_1 + \mathbf{q}| - k_F)}{\omega_q(\mu_1^2 + W_1^2)} \right. \\ \left. + \frac{2\mu_1 \mu_2 \Theta(|\mathbf{p}_1 + \mathbf{q}| - k_F) \Theta(|\mathbf{p}_2 + \mathbf{q}| - k_F)}{(\mu_1^2 + W_1^2)(\mu_2^2 + W_2^2)} \right. \\ \left. + \frac{2W_1 W_2 \Theta(W_1) \Theta(W_2) \Theta(|\mathbf{p}_1 + \mathbf{q}| - k_F) \Theta(|\mathbf{p}_2 + \mathbf{q}| - k_F)}{(\mu_1^2 + W_1^2)(\mu_2^2 + W_2^2)} \right], \quad (6d)$$

where

$$\nu = \epsilon_{|\mathbf{k} - \mathbf{q}|} + \omega_q - \epsilon_k,$$

$$\mu_i = \epsilon_{|\mathbf{p}_i + \mathbf{q}|} - \omega_q - \epsilon_{p_i},$$

$$W_i = \Sigma(|\mathbf{p}_i + \mathbf{q}|) - \Sigma(p_i).$$

P is the Cauchy principal part, Θ is the step function, and $\Sigma(p_i)$ is the imaginary part of the self-energy on the energy shell.

All terms except (6b) can be evaluated numerically and give finite and smooth contributions to the APS intensity. Attempts to integrate (6b) lead to a logarithmic divergence. Because of the recoilless nature of the suddenly created core hole, the simple addition of a core-hole self-energy does not remove this divergence.¹ The procedure for handling this divergence is similar to that done for the photoemission case⁵ by separating out the static part of the effective interaction in (6b). While the remaining dynamic single-particle contribution is smooth and well behaved, the static part is responsible for the anomalous behavior at the threshold, known as the edge effect. It is necessary to handle this term using a one-body (ND) type formalism, where one relates the scattering of the conduction electrons by the suddenly created core hole in terms of their phase shifts (δ_l) near the Fermi surface. The ND theory also takes into account scattering of the final-state

electrons by the core hole. This requires that we also separate out the static part of the effective interaction in the third term of (6d) to avoid double counting.

In II this electron-core hole scattering was handled by an extension of the Laramore APS edge theory. The Laramore theory was extended to regions away from the edge by an approach first formulated by Longe⁸ to deal with the edge structures in x-ray emission and absorption spectra. While the Laramore theory, based on the ND formalism, requires that a separable core hole-electron scattering potential be used, the Longe theory allows the use of a realistic nonseparable potential. This is an essential requirement in dealing with regions away from the edge. In II the potential used is

$$V(q) = \frac{V_{\text{ps}}(q)}{\epsilon(q)}, \quad (7)$$

where $\epsilon(q)$ is the static Lindhard dielectric function and V_{ps} is the Ashcroft pseudopotential⁹

$$V_{\text{ps}}(q) = \frac{4\pi e^2}{q^2} \cos(qR_c^*), \quad (8)$$

where R_c^* is the cutoff radius modified by the absence of the core electron.^{9,8}

To handle the edge calculations we have used a linear-

response theory, where the edge intensity is written in terms of the linear-response function (F) as

$$I_I(\epsilon_k) = \frac{\text{Re}}{\pi} \int_0^\infty ds e^{i(\epsilon_k + E_c)s} F(s), \quad (9)$$

where the response function is written in the interaction picture as

$$F(s) = \frac{\langle \phi | T \{ H_I^\dagger(s) H_I(0) U(\infty, -\infty) \} | \phi \rangle}{\langle \phi | U(\infty, -\infty) | \phi \rangle}. \quad (10)$$

In Eq. (10), ϕ is the ground-state wave function, H_I is the interaction Hamiltonian describing the core hole–electron scattering, U is the time translation operator, and T is the Dyson time-ordering product. The details of the edge calculation along with its extension away from the edge is given in II. Thus by combining the S - and T -matrix formalism with the extension of the ND-Laramore edge theory we have developed a formulation of the APS intensity which is finite away from the edge and valid at all energies.

III. RESULTS AND DISCUSSION

Numerical results for the $2p$ and $1s$ derivative spectra of Al are shown in Figs. 2(a) and 2(b), respectively. These figures combine the contributions of the previously calculated plasmon structures² and the edge structure³ with the contribution of the single-particle excitations calculated in the present article. It is found that the single-particle excitation spectra (without the edge terms) are smooth and without structure. The divergent behavior at the threshold³ and the structure at the threshold for plasmon production² are not significantly altered by this single-particle contribution. However, with the addition of the latter, the change in concavity at the energy corresponding to the highest frequency for plasmon production (plasmon cutoff frequency) is found to become less pronounced than the one shown in Figs. 6 and 7 of I. As there are other structures present in the APS due to band-structure and extended fine-structure effects, this subtle feature would be obscured and may not show up in a spectrum measured with the usual experimental resolution.¹⁰ However, it may be noted that in a $1s$ x-ray photo-

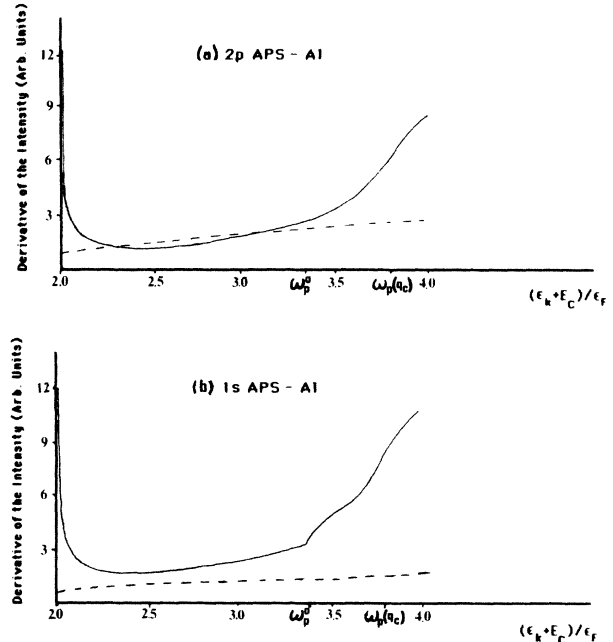


FIG. 2. The calculated (a) $2p$ and (b) $1s$ APS spectrum of Al from the first-order S -matrix theory and edge formalism. Included are the first plasmon satellite, threshold singularity, and modification of the main band due to single-particle excitations. The dashed line in each figure is the one-electron band shape.

absorption (XPA) spectra experiment by Sénémaud,¹¹ a careful reexamination of the XPA line shape in the neighborhood of the plasmon cutoff frequency revealed a feature predicted by Bose and Longe¹² and it is of the same origin as the feature we have predicted at the cutoff frequency in the APS.

ACKNOWLEDGMENTS

One of the authors (P.L.) is grateful to the Fonds National de la Recherche Scientifique, Belgium and the Coopération Scientifique Internationale, Belgium, for financial support.

¹R. Patrick, Ph.D. thesis, Drexel University, 1986.

²R. Partrick, S. M. Bose, and P. Longe, Phys. Rev. B **32**, 3507 (1985).

³R. Patrick, S. M. Bose, and P. Longe, Phys. Rev. B **32**, 6286 (1985).

⁴D. Chastenet and P. Longe, Phys. Rev. Lett. **44**, 91 (1980).

⁵S. M. Bose, P. Kiehm, and P. Longe, Phys. Rev. B **23**, 712 (1981).

⁶G. E. Laramore, Phys. Rev. Lett. **27**, 1050 (1971).

⁷P. Nozières and C. T. De Dominicis, Phys. Rev. **178**, 1097

(1969).

⁸P. Longe, Phys. Rev. B **8**, 2572 (1973).

⁹N. W. Ashcroft, Phys. Lett. **23**, 48 (1966); J. Phys. C **1**, 232 (1968).

¹⁰Recent unpublished work by J. C. Fuggle *et al.* reports that there is no significant structure at the plasmon cutoff frequency in the $1s$ derivative spectra of Al.

¹¹C. Sénémaud, Phys. Rev. B **18**, 3929 (1978).

¹²S. M. Bose and P. Longe, Phys. Rev. B **18**, 3921 (1978).